


---

This is the **accepted version** of the journal article:

Pol, Roberto; Moya Lara, Ana; Gabriel, Gemma; [et al.]. «Inkjet-Printed Sulfide-Selective Electrode». Analytical chemistry, Vol. 89, Issue 22 (October 2017), p. 12231-12236. DOI 10.1021/acs.analchem.7b03041

---

This version is available at <https://ddd.uab.cat/record/264078>

under the terms of the  **IN**  
COPYRIGHT license

## Inkjet-printed sulfide-selective electrode

Roberto Pol<sup>†</sup>, Ana Moya<sup>‡,§</sup>, Gemma Gabriel<sup>‡,§</sup>, David Gabriel<sup>#</sup>, Francisco Céspedes<sup>†</sup>, Mireia Baeza<sup>†\*</sup>

<sup>†</sup> Departament of Chemistry, Faculty of Science, Edifici C-Nord, Universitat Autònoma de Barcelona, Carrer dels Til·lers, 08193 Bellaterra (Cerdanyola del Vallès), Barcelona, Spain

<sup>‡</sup> Instituto de Microelectrónica de Barcelona, IMB-CNM (CSIC), Esfera UAB, Campus Universitat Autònoma de Barcelona, 08193 Bellaterra (Cerdanyola del Vallès), Barcelona, Spain

<sup>§</sup> CIBER de Bioingeniería, Biomateriales y Nanomedicina (CIBER-BBN), Campus Universitat Autònoma de Barcelona, 08193 Bellaterra (Cerdanyola del Vallès), Barcelona, Spain

<sup>#</sup> GENOCOV Research Group, Department of Chemical, Biological and Environmental Engineering, School of Engineering, Universitat Autònoma de Barcelona, Carrer de les Sitges, 08193 Bellaterra (Cerdanyola del Vallès), Barcelona, Spain

**KEYWORDS:** Sulfide detection, inkjet printing, second kind electrode, ion-selective electrode

**ABSTRACT:** Inkjet printing technology has emerged as an alternative manufacturing method for low-cost production of electrodes. Despite significant progress, there is still a lack in the production of ion-selective electrodes. Herein, the two-step fabrication of the first inkjet-printed sulfide-selective electrode (IP SSE) is described. The two-step fabrication consists of printing a silver path followed by an electrochemical deposition of sulfide to produce a second kind electrode (Ag/Ag<sub>2</sub>S). The performance of this novel device was tested using potentiometric measurements. Nernstian response ( $-29.4 \pm 0.3$  mV/decade<sup>-1</sup>) was obtained within concentrations of 0.03–50 mM with a response time of  $\sim 3$  s. Furthermore, river/sea-spiked environmental samples and samples from a bioreactor for sulfate reduction to sulfide were measured and compared against a commercial sensor giving no significant differences. The IP SSE described in this work showed good reproducibility and durability during daily measurements over 15 days without any special storage conditions. Considering all the current challenges in inkjet-printed ion-selective electrodes, this different fabrication approach opens a new perspective for mass production of all-solid state ion-selective electrodes.

### INTRODUCTION

Modern manufacturing processes have left wide-spread hazardous compounds across the globe. Sulfide, which is present in several waste waters, have gain significant attention within the scientific community due to its toxicity.<sup>1</sup> The over exposure of workers involved in decontamination processes in sewage treatment plants and the direct impact in rivers and streams has triggered the alarms. Therefore, production of durable, fast and robust sensing platforms to track sulfide concentration across the environment has become a global concern.

Manufacturing of electrochemical sensors has represented a hot topic during decades.<sup>2,3</sup> Traditionally, electrochemical sensors were home-made using metal wires for their subsequent use in the laboratory. Those hand-crafted sensors lack certain requirements (e.g. reproducibility, repeatability, robustness) regarding the performance of the analytical assays. Moreover, their operation-

al configuration makes them a bad choice for on the field analyses. Nowadays, breakthrough technologies, such as microfabrication and printing techniques have led to more automated sensor fabrication procedures.<sup>4,5</sup> With these technologies, typical requirements, such as reproducibility and repeatability are met in a miniaturized fashion, which in turns allow them to be used in broader situations. Therefore, their potential is spotted and the feasibility of its commercialization has increased exponentially.

Among others, inkjet printing technology has emerged as a standard method for production of low-cost electronics. Inkjet printing constitutes a contactless, additive process with the capability to deposit microdroplets of ink on a substrate following a digitalized predefined pattern.<sup>6,7</sup> Ink formulations are composed by materials that can be dispersed, suspended or dissolved in a liquid with defined properties (viscosity, surface tension and boiling point). In fact, electrical conductive paths can be inkjet-

printed from a wide variety of materials, from metals to conductive polymers.<sup>8,9,10</sup> Moreover, different substrates can be used depending on the final application of the electronics. In this context, flexible substrates excel thanks to their adaptability to different situations and their cost-efficiency.<sup>11,12</sup> Overall, inkjet printing allows *in-situ* digital modification of the complex printed patterns removing the need for mask, outstripping other techniques with that dependence. The use of mask-less deposition not only helps with the capability of changing the motifs on demand during the prototyping process, but also leads to an efficient use of materials and waste elimination.<sup>13</sup> With this outstanding technology available, the challenges to control all the parameters that affect the reproducibility and durability of the sensors are addressed alongside with achieving a substantial fall in prices. Thanks to all those benefits inkjet printing technology give, techniques such as potentiometry are coming back to play an important role.

Traditionally, one of the most used sensors so far are ion-selective electrodes due to their operational simplicity and reliability.<sup>14,15</sup> Their capability to measure a defined ion in highly complex matrices with high selectivity makes them appealing for any required situation. This kind of electrodes measure potential differences associated with permselective mass transfer across a phase boundary.<sup>16</sup> Depending on the nature of this phase boundary, ion-selective sensors are classified in different groups (glass membrane, crystalline membrane and polymeric membrane).<sup>17</sup> Over the above phase boundaries, the one that has attracted more attention is the polymeric matrix. For instance, Sjöberg et al.<sup>18</sup> described the fabrication of a potassium-selective electrode by means of inkjet printing. Authors demonstrate the importance of the methodology used for deposition of a homogeneous solid contact (poly(3,4-ethylenedioxythiophene) polystyrene sulfonate) between the ion-selective polymeric membrane and the transducer (gold). Another daily used worldwide potentiometric sensor (pH) has also been extensively investigated. Qin et al.<sup>19</sup> successfully developed a Pd-based printable ink and described the fabrication of a Pd/PdO inkjet-printed electrode with excellent response against  $H^+$ . Although many efforts have been done to produce polymeric and glass-based potentiometric sensors, there is a gap in the production of second and third kind ion-selective electrodes.

Herein, the two-step fabrication of the first second kind Ag/Ag<sub>2</sub>S inkjet-printed sulfide-selective electrode (IPSSE) is described. Despite the challenges, the device was successfully fabricated by printing a silver path followed by an electrochemical deposition of sulfide. Interestingly, advantage of the nature of the conductive printed ink was taken. The morphology of the device was characterized by scanning electron microscopy (SEM) coupled with energy-dispersive X-ray analysis. Furthermore, the electrochemical performance of the sensor was evaluated with potentiometric measurements in standard solutions and in real environmental and biotechnological matrices.

## EXPERIMENTAL SECTION

**Materials and chemicals.** All chemicals were commercially available and were used without further purification. Sodium sulfide nonahydrate (98%, Na<sub>2</sub>S·9H<sub>2</sub>O), sodium hydroxide (98%, NaOH), sodium thiosulfate (99%, Na<sub>2</sub>S<sub>2</sub>O<sub>3</sub>) and starch were purchased from SigmaAldrich. L(+)-ascorbic acid (99%), potassium iodide (99%, KI) and potassium iodate (99%, IO<sub>3</sub>K) were purchased from Panreac (Spain).

Silver nanoparticle ink (PE410) was purchased from DuPont, Korea, and an SU8 ink (2002) was purchased from MicroChem, USA. Teonex Polyethylene Naphthalate PEN films (Q65HA) with a thickness of 125 μm and a surface pre-treatment for improved adhesion was purchased from DuPont Teijin Films.

**Sulfide standard solutions and standardization.** Aqueous solutions were prepared employing deionized Milli-Q water (180 MΩ·cm<sup>-1</sup>). Stock solution of S<sup>2-</sup> (1 M S<sup>2-</sup>) was prepared by dissolving 24.5 g of Na<sub>2</sub>S·9H<sub>2</sub>O in 100 mL of a 1 M NaOH solution. Standard solutions of S<sup>2-</sup> were daily prepared by dilution of the stock solution in sulfide antioxidant buffer (SAOB). The SAOB was prepared by mixing 40 g L<sup>-1</sup> (1 M) of NaOH (increasing the pH up to 14 which ensures that the predominant specie present in solution of the acid-base equilibrium will be S<sup>2-</sup>) and 10.1 g L<sup>-1</sup> (0.05 M) of ascorbic acid (which act as an antioxidant to avoid the presence of other sulfur oxidized forms).

The determination of the real concentration of the stock solution of sulfide was performed applying an iodometric method according to the Standard methods.<sup>20</sup>

Briefly, standardization of a Na<sub>2</sub>S<sub>2</sub>O<sub>3</sub> with I<sub>3</sub><sup>-</sup> takes place. Then, Na<sub>2</sub>S<sub>2</sub>O<sub>3</sub> standardized solution is used to determine the iodine produced by the reaction of sulfide with iodide.

**Electrode fabrication: Printing procedure and sulfide electrodeposition.** The two-step fabrication (Figure 1) of the first IPSSE consists of printing a silver path **and an insulator** followed by an electrochemical deposition of sulfide to produce a second kind electrode (Ag/Ag<sub>2</sub>S).

Silver electrodes were prepared by using a drop-on-demand inkjet printer (DMP-2831 Dimatix Fujifilm, Santa Clara, USA) and a disposable cartridge (DMC-x<sup>®</sup>11610) containing 16 individually addressable nozzles with nominal droplet volumes of 10 pL. The printing processes were carried out in a standard laboratory environment in ambient condition. The IPSSE were printed over a flexible and transparent PEN substrate using a commercial available Ag and SU8 inks. Printing parameters (cartridge temperature, piezoelectric nozzle voltage, frequency, etc.) were optimized for both employed inks. The active work-

ing electrode area delimited by the SU8 insulator is 2 mm per 1 mm (further details, Figure S1).

Previously to begin the printing steps, silver and SU8 inks behavior was studied by printing a predefined line pattern over the PEN substrate. This test print pattern allows to know which is the drop spacing (DS) required to print a continuous line, and so the thickness and width of lines. These parameters basically depend on the surface energy of each ink on the desired substrate, so it is mandatory to do it before each printing. In the first step of the printing (Figure 1A) the active working electrode area, track and pad were printed with Ag ink using a DS of 30  $\mu\text{m}$ . During printing of the silver layer, the substrate temperature was set to 40  $^{\circ}\text{C}$  in order to promote the beginning of evaporation of the ink carrier and thus to increase the pattern resolution. The completely evaporation was done outside the printer, at 100  $^{\circ}\text{C}$  during 10 min using a hotplate. The inks contain different solvents, so, this drying step is necessary to achieve that all solvent molecules absorbed on the nanoparticles are completely removed. After the drying step, the patterns were sintered for 20 min at 140  $^{\circ}\text{C}$ . This sintering step is considered necessary to lower the resistivity of the ink, and although high temperatures can achieve better conductivities, with the selected sintering conditions, it was achieved a resistivity down to 10  $\mu\Omega\cdot\text{cm}$ . Afterwards, the insulator layer was printed over the silver tracks (Figure 1B) to precisely define the active area of the working electrode. The insulating SU8 UV curable ink, was printed using a DS of 15  $\mu\text{m}$ . The SU8 achieves a high chemical resistance and a high thermal stability after a soft bake at 100  $^{\circ}\text{C}$  for 5 min and a UV curing of 15 seconds where the layer polymerizes by cross-linking.

The electrochemical deposition (Figure 1C) was carried out by a potentiostat/galvanostat AUTOLAB (PGSTAT204, Eco Chemie, Utrecht, The Netherlands) using chronoamperometry mode applying a potential of 0.7 V during 5 s under non-stirring conditions. A double junction reference electrode Ag/AgCl Orion 900200 (Thermo Electron Corporation, Beverly, MA, USA), a platinum-based electrode Crison (Crison Instruments, Alella, Barcelona, Spain) and the inkjet-printed silver electrode were used as reference, counter and working electrodes, respectively. Electrolytic solution used for electrodeposition was a 0.1 M  $\text{S}^{2-}$  solution with adjusted pH to 14 using NaOH.

**Electrode characterization.** Morphological changes produced by the electrodeposition were observed by SEM using a MerlinZeiss microscope operated at 5 kV. Samples for SEM were prepared by simply sticking the substrate onto the holder with carbon tape. The elemental composition was determined by Energy Dispersive X-ray Spectroscopy (EDX) at a voltage of 15 kV.

Evaluation of the electrochemical performance was done by a potentiostat/galvanostat AUTOLAB

(PGSTAT204) using chronopotentiometry under constant stirring conditions. The IPSSE was used against a double junction reference electrode Ag/AgCl Orion 900200. All calibrations performed in this research are made in batch condition with subsequent addition (over 25 mL of SAOB) of standards  $\text{S}^{2-}$  solutions.

**Sampling, spiking and determination in real samples.** River and sea water samples were collected following ISO 5667-6:2014 and ISO 5667-9:1992, respectively (further details in Table S1). Subsequently, both samples were filtered through a Millex 0.45  $\mu\text{m}$  filter and conditioned by dilution with twice concentrated SAOB (1:1) to increase the pH up to 14. Afterwards, both solutions were spiked with the same amount of  $\text{S}^{2-}$  from the stock solution to fit in the middle of the calibration curve. In addition, process samples were collected from the outlet sampling port of a 2L upflow anaerobic sludge blanket reactor (UASB) performing anaerobic sulfate reduction to sulfide using crude glycerol as electron donor. UASB performance at the time of sampling corresponded to almost complete conversion of a sulfate concentration of 0.25  $\text{kg S m}^{-3}$ . Samples from the reactor were filtered through a Millex 0.45  $\mu\text{m}$  filter and conditioned by dilution with twice concentrated SAOB (1:1).

Measurements were done by simply immerse the IPSSE and the double junction reference electrode in the solutions. The results obtained were compared against a commercial available Orion 9616BNWP (Thermo Electron Corporation, Beverly, MA, USA) sulfide-selective electrode using a SB90M5 potentiostat (SympHony<sup>TM</sup>, VWR).

## RESULTS AND DISCUSSION

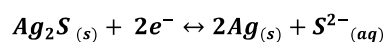
Potential applied in the electrodeposition step constitute a key factor in the production of durable Ag<sub>2</sub>S films. The first electrochemical deposition attempt was to use 1 V but the film was taken off after rinsing the electrode. This fact could be explained by the loss of cohesion between layers due to the overproduction of oxygen bubbles caused by the water oxidation reaction for potentials around 1 V. Then, different potentials were applied (0.9 and 0.8 V) until an optimal potential of 0.7 V was found (Figure S2). Another factor that was crucial is the electrodeposition time. Long times (+30 s) causes the formation of Ag/Ag<sub>2</sub>S until the interface of the polymeric support, decreasing the cohesion and falling off after rinsing step. Therefore, 5 seconds was chosen as the electrodeposition time that gave a robust Ag/Ag<sub>2</sub>S layer (Figure S3).

The successful electrochemical deposition of the as-fabricated IPSSE can be easily discerned by naked eye (Figure 2). A change from a pale grey (Figure 2A) to black

(Figure 2B) is evidenced. Furthermore, SEM micrographs show a change in the morphology of the electrode. On the one hand, the inkjet-printed silver electrode (Figure 2A center) exhibits a granular surface typical of an inkjet printing process of nanosized silver particles.<sup>21</sup> On the other hand, the IPSSE presents a transformation at the external surface to a coral-like shape after the electrochemical deposition (Figure 2B center).

EDX demonstrates the presence of S after the electrochemical deposition (Figure 2B right). The EDX data showed the appearance of two peaks at 2.3 and 2.7 KeV corresponding to S aside from the Ag peaks (3.1 and 3.3 KeV) once the deposition occurs.

The IPSSE must accomplish several statements prior to its use in real samples. A Ag<sub>2</sub>S-rich surface for the ion-to-electron transduction based on the following redox reaction



in which the redox potential is described by the Nernst equation:

$$E = E^0 - \frac{59.16}{n} \log[\text{S}^{2-}]$$

where  $E_0$  is the standard potential,  $n$  is the number of electrons involved in the redox reaction and  $[\text{S}^{2-}]$  is the activity of  $\text{S}^{2-}$  ions in solution. Therefore, the theoretical sensitivity of the sensor should be -29.58 mV/decade<sup>-1</sup>.

Thus, the electroanalytical performance of the as-fabricated IPSSE was extensively studied. Figure 3A shows an example of the time trace of the potentiometric response during consecutive additions (every 30 s) of sulfide. The corresponding calibration curve obtained for three subsequent calibrations is shown in Figure 3B. The calibration curve exhibit a Nernstian response of -29.4±0.3 mV/decade (±confidence interval at 95%) between 0.03-100 mM with a detection limit of 0.01 mM (calculated by intersection of the slope and the asymptote)<sup>22</sup> in concordance with the expected value for these kind of electrodes.<sup>23</sup> Through all calibration curve data, the confidence interval (y error) cannot be discerned thanks to its high repeatability. Is it worth noting that the IPSSE also shows a prompt response of 3 s (Figure S4).

Generally, inkjet-printed electrodes are designed and produced to be disposable due to their poor mechanical properties as they detach from the surface and heavily suffer surface scratching affecting their performance. With this fact in mind, the durability of the IPSSE was tested over days (Figure 3C). Systematically, durability experiments were carried with daily triplicate calibrations. Surprisingly, the IPSSE was able to be reused for at

least 15 days with no extent of the slope greater than 3-folds the standard deviation (of each daily calibration, both dashed red line) of the theoretical value (-29.58 mV/decade, red line) in the same concentration range.

Although second kind electrodes are well-known for their specificity towards the ions that compose the electrode, a simple experiment to ensure the selectivity towards  $\text{S}^{2-}$  over a cocktail of ions ( $\text{K}^+$ ,  $\text{Na}^+$ ,  $\text{Cl}^-$  and  $\text{SO}_4^{2-}$ ) was performed. Three calibration curves with  $\text{S}^{2-}$  in highly concentrated background of common ions (10 mM) were done (Figure S5). Although slight differences in the slope existed, no remarkable difference in the limit of detection (from 0.01, without interfering ions; to 0.02, with interfering ions) was found whatsoever.

Other factors that have to be studied to guarantee the validation of a method are repeatability and reproducibility. Repeatability was tested by the same analyst in a short period of time. The measurements were done preparing 10 beakers containing the same solution (at three different concentrations of the calibration curve) and then the electrodes (working and double junction reference) were systematically immerse and rinsed with copious amounts of water between every measurement. Results of this procedure are summarized in Table S2. Confidence intervals (95%) for each point were below 1 mV, which is in agreement with precision measured with other ion-selective electrodes.<sup>23</sup> In this particular case, the reproducibility was studied in terms of the fabrication process. Three different full fabrication processes separated in days were done. Results of the calibration curves by triplicate (of each one) gave a mean Nernstian response of 30±2 mV/decade (±confidence interval at 95%). Summarizing, the fabrication process successfully provided reliable sulfide-selective electrodes with potential to be used in real matrices.

The performance of the new IPSSE was tested towards real samples. Really different samples were chosen to showcase the performance of the sensor in different domains. Common river and sea water samples were chosen as environmental matrices, while samples from the outlet of the UASB reactor were selected as industrial matrices. Table 1 show the comparison between the  $\text{S}^{2-}$  concentrations obtained with the IPSSE and the obtained with a commercial available sensor (calibration curve, Figure S6). Results show that the concentrations of each sample found with both sensors do not differ significantly at a confidence level of 95% (statistics detailed in Supporting Information Statistics Section). In the case of environmental-spiked samples (diluted in the same manner), they were also measured without the presence of spiked sulfide by both sensors, giving concentrations below the detection limits. Furthermore, the recovery rates were



calculated, 95-96% and 86-88% rates were achieved by the IPSSE and the commercial, respectively (Table 1). Overall, the described fabrication methodology demonstrated to be capable to produce sulfide-selective electrodes (for  $S^{2-}$  sensing purposes) which can compete alongside a commercial available one.

Traditionally, sulfide was measured using potentiometry. Nonetheless, the phase boundary used was a crystalline membrane. The typical procedure to produce that crystalline membrane was a precipitation of  $Ag_2S$  from their respective ionic salts and then a pellet is produced by applying high pressure to the resulting powder.<sup>24</sup> This kind of potentiometric electrodes can encounter some problems (electrical contact, Galvani potential difference, mechanical influences...) in their tedious production.<sup>25</sup> Moreover, they can be hardly miniaturized, limiting their practical applications. The trend nowadays, is to produce simple optical sensors for naked-eye quantification. For instance, Kang et al.<sup>26</sup> developed a G-Quadruplex DNAzyme which contains hemin that in the presence of sulfide its activity is inhibited. Another simple sensor was reported by Rosolina et al.<sup>27</sup> in which a paper containing bismuth hydroxide changes the color in the presence of sulfide due to  $Bi_2S_3$  precipitation. It is worth noting that sensors that contain biomolecules undergo degradation (sometimes caused by the interaction with compounds of the samples) and require special storage conditions. Moreover, in most scenarios optical sensors encounter several problems with environmental samples that contain particles (or color) that disperse light.<sup>28</sup> Therefore, the fabrication methodology proposed in this manuscript excels providing functional sulfide sensors in a miniaturized fashion that have demonstrated to be useful in a wide variety of situations.

Apart from this breakthrough fabrication process, a less sophisticated and more hand-crafted process was briefly tested. The inkjet printer was replaced by a nail brusher and the electrochemical oxidation by long term spontaneous deposition. A silver path was manually drawn and sintered. Then, milling conditions (Ag is oxidized in basic media) of the electrolytical solution allow the deposition of  $Ag/Ag_2S$  in 1 day. Surprisingly, the electrode gave a Nernstian response. This non-controlled test could constitute a game changer in the self-production of electrodes at home.

## CONCLUSIONS

The fabrication and the electrochemical performance of the first IPSSE is described. The IPPSE was successfully fabricated by printing a silver path followed by an electrochemical deposition of sulfide. Although this fabrication

procedure was composed by two consecutive completely different techniques, further efforts could be done to try to produce an inkjet printable  $Ag_2S$  ink which will reduce the required equipment. Nonetheless, the fabrication process demonstrates high reproducibility and reliability. An expected Nernstian response of  $-29.4 \pm 0.3$  mV/decade was obtained within concentrations of 0.03-50 mM with a short response time (3 s). Furthermore, the IPSSE was tested with real samples and gave results in agreement with a commercial available one. Taking into account the challenges inkjet-printed ion-selective face, this different fabrication approach could open new ways of mass production of all-solid state ion-selective sensors.

Although, in this manuscript is showcased the fabrication methodology of a single type of ion-selective electrode, the potential of inkjet printing to produce not only other potentiometric electrodes but also other kind of functional miniaturized electronics in a simple way should be highlighted.

## AUTHOR INFORMATION

### Corresponding Author

\* Departament of Chemistry, Faculty of Science, Edifici C-Nord, Universitat Autònoma de Barcelona, Carrer dels Til·lers, 08193 Bellaterra (Cerdanyola del Vallès), Barcelona, Spain.

E-mail: mariadelmar.baeza@uab.cat

### Author Contributions

The manuscript was written through contributions of all authors. All authors have given approval to the final version of the manuscript.

## ACKNOWLEDGMENTS

R. Pol would like to acknowledge Universitat Autònoma de Barcelona (UAB) for the PIF grant. Authors would also like to thank the financial support from the CTQ2015-69802-C2-1-R research project from the Spanish Ministerio de Economía y Competitividad y Fondo Europeo de Desarrollo Regional (MINECO/FEDER, UE). Authors also want to thank the support of the Generalitat de Catalunya to GENOCOV (2104-SGR-1255).

## ABBREVIATIONS

DS, drop spacing; EDX, Energy-dispersive X-ray spectroscopy; IPSSE, Inkjet-printed sulfide-selective electrode; SEM, Scanning electron microscopy; UASB, Upflow anaerobic sludge blanket reactor.

## REFERENCES

- (1) Nooredeen Abbas, M.; Radwan, A.-L.; Nawwar, G.; Zine,

- N.; Errachid, . A. *Anal. Methods* **2015**, 7 (3), 930–942.
- (2) Privett, B. J.; Shin, J. H.; Schoenfisch, M. H. *Electrochemical Sensors. Anal. Electrochem.* **2010**, 82, 4723–4741.
- (3) Kimmel, D. W.; Leblanc, G.; Meschievitz, M. E.; Cliffel, D. E. *Anal. Chem.* **2012**, 84 (2), 685–707.
- (4) Hughes, G.; Westmacott, K.; Honeychurch, K. C.; Crew, A.; Pemberton, R. M.; Hart, J. P. *Analyses. Biosensors* **2016**, 6, 50.
- (5) Abdulbari, H. A.; Basheer, E. A. M. *ChemBioEng Rev.* **2017**, 4 (2), 92–105.
- (6) Gao, M.; Li, L.; Song, Y. Inkjet Printing Wearable Electronic Devices. *J. Mater. Chem. C* **2017**, 5, 2971–2993.
- (7) Guo, Y.; Patanwala, H. S.; Bognet, B.; Ma, A. W. K. *Rapid Prototyp. J.* **2017**, 23 (3), 562–576.
- (8) Kell, A. J.; Paquet, C.; Mozenon, O.; Djavani-Tabrizi, I.; Deore, B.; Liu, X.; Lopinski, G. P.; James, R.; Hettak, K.; Shaker, J. *ACS Appl. Mater. Interfaces* **2017**, 9, 17226–17237.
- (9) Torrisi, F.; Hasan, T.; Wu, W.; Sun, Z.; Lombardo, A.; Kulmala, T. S.; Hsieh, G. W.; Jung, S.; Bonaccorso, F.; Paul, P. J. *ACS Nano* **2012**, 6 (4), 2992–3006.
- (10) Ngamna, O.; Morrin, A.; Killard, A. J.; Moulton, S. E.; Smyth, M. R.; Wallace, G. G. *Langmuir* **2007**, 23 (16), 8569–8574.
- (11) Zhang, G.; Hui, H. Y.; Chu, P. H.; Yuan, Z.; Chang, R.; Risteen, B.; Yang, H.; Reichmanis, E. *Chem. Mater.* **2016**, 28 (23), 8475–8479.
- (12) Root, S. E.; Savagatrup, S.; Printz, A. D.; Rodriguez, D.; Lipomi, D. J. *Chem. Rev.* **2017**, acs.chemrev.7b00003.
- (13) Moya, A.; Gabriel, G.; Villa, R.; Javier, F. *Curr. Opin. Electrochem.* **2017**, (In press).
- (14) Hu, J.; Stein, A.; Bühlmann, P. *TrAC - Trends Anal. Chem.* **2016**, 76, 102–114.
- (15) Zuliani, C.; Diamond, D. *Electrochim. Acta* **2012**, 84, 29–34.
- (16) Bu, P. *Chem.. Rev.* **1998**, 2665 (97), 1593–1688.
- (17) Bakker, E.; Bühlmann, P.; Pretsch, E. *Electroanalysis* **1999**, 11 (13), 915–933.
- (18) Sjöberg, P.; Määtänen, A.; Vanamo, U.; Novell, M.; Ihalainen, P.; Andrade, F. J.; Bobacka, J.; Peltonen, J. *Sensors Actuators, B Chem.* **2016**, 224, 325–332.
- (19) Qin, Y.; Alam, A. U.; Howlader, M. M. R.; Hu, N.; Deen, M. J. **2016**, 26, 4923–4933.
- (20) American Public Health Association. *Standard Methods: For the Examination of Water and Wastewater*, 22nd ed.; Washington, DC, 2012.
- (21) da Silva, E. T. S. G.; Miserere, S.; Kubota, L. T.; Merkoçi, A. *Anal. Chem.* **2014**, 86 (21), 10531–10534.
- (22) Bakker, E.; Bühlmann, P.; Pretsch, E. *Chem. Rev.* **1997**, 97 (8), 3083–3132.
- (23) Novell, M.; Parrilla, M.; Crespo, A.; Rius, F. X.; Andrade, F. J. *Anal. Chem.* **2012**, 84 (11), 4695–4702.
- (24) Redondo, R.; Machado, V. C.; Baeza, M.; Lafuente, J.; Gabriel, D. *Anal. Bioanal. Chem.* **2008**, 391, 789–798.
- (25) Gründler, P. *Chemical Sensors*; Springer: Berlin, 2006.
- (26) Kang, S.; Oh, J.; Han, M. S. *Dye. Pigment.* **2017**, 139, 187–192.
- (27) Rosolina, S. M.; Thomas, S.; Xue, Z. *Anal. Chem.* **2016**, 88, 1553–1558.
- (28) Pol, R.; Céspedes, F.; Gabriel, D.; Baeza, M. *TrAC - Trends Anal. Chem.* **2017**, 95, 62–68.

# Inkjet-printed sulfide-selective electrode

Roberto Pol<sup>†</sup>, Ana Moya<sup>‡,ξ</sup>, Gemma Gabriel<sup>‡,ξ</sup>, David Gabriel<sup>#</sup>, Francisco Céspedes<sup>†</sup>, Mireia Baeza<sup>†\*</sup>

<sup>†</sup> Departament of Chemistry, Faculty of Science, Edifici C-Nord, Universitat Autònoma de Barcelona, Carrer dels Til·lers, 08193 Bellaterra (Cerdanyola del Vallès), Barcelona, Spain

<sup>‡</sup> Instituto de Microelectrónica de Barcelona, IMB-CNM (CSIC), Esfera UAB, Campus Universitat Autònoma de Barcelona, 08193 Bellaterra (Cerdanyola del Vallès), Barcelona, Spain

<sup>ξ</sup> CIBER de Bioingeniería, Biomateriales y Nanomedicina (CIBER-BBN), Campus Universitat Autònoma de Barcelona, 08193 Bellaterra (Cerdanyola del Vallès), Barcelona, Spain

<sup>#</sup> GENOCOV Research Group, Department of Chemical, Biological and Environmental Engineering, School of Engineering, Universitat Autònoma de Barcelona, Carrer de les Sitges, 08193 Bellaterra (Cerdanyola del Vallès), Barcelona, Spain

## FIGURE CAPTION

**Figure 1.** Scheme of the fabrication of the IPSSE: Inkjet printing of Ag paths (A), insulator printing (B) and electrodeposition step (C).

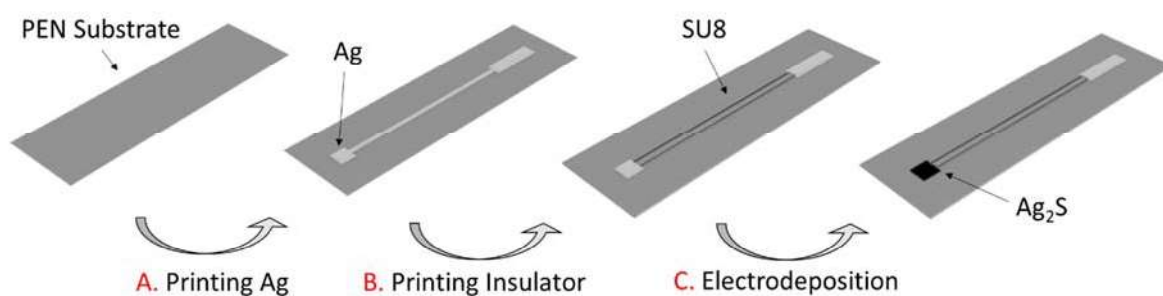
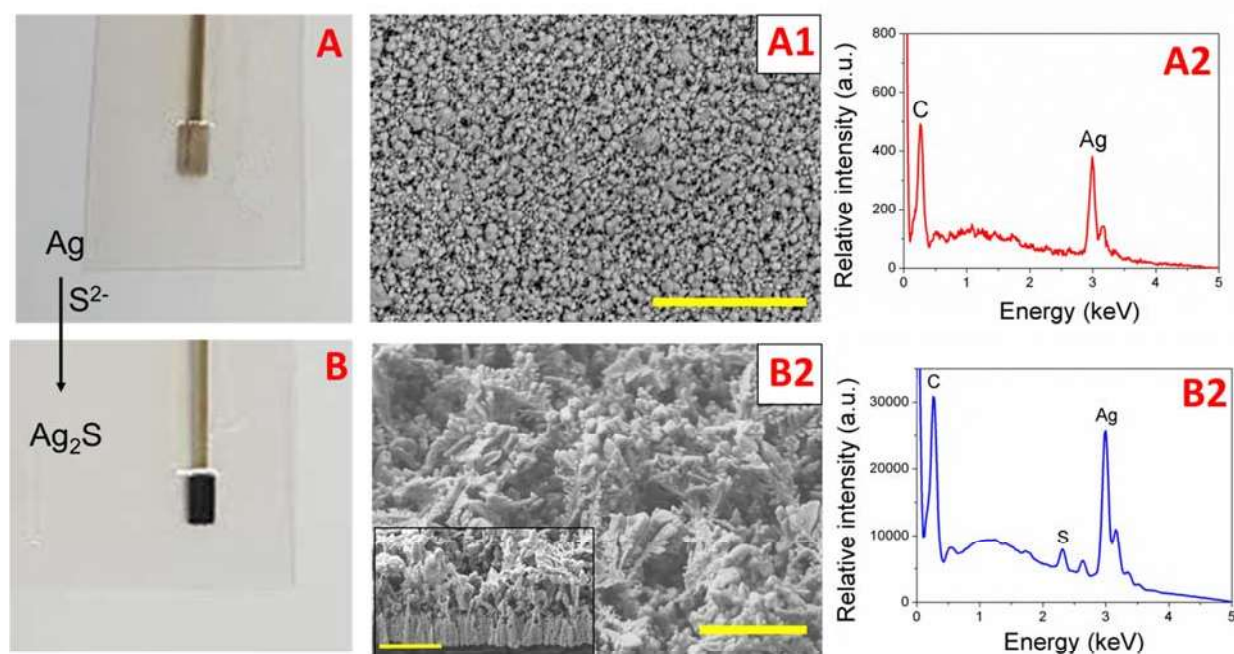
**Figure 2.** Ag inject printing electrode (A), SEM micrographs (A1) and EDX (A2). Ag/Ag<sub>2</sub>S electrode (B), SEM micrographs (B1) and EDX for Ag/Ag<sub>2</sub>S electrode (B2); scale bar = 2 μm.

**Figure 3.** Response of the Ag/Ag<sub>2</sub>S electrode for S<sup>2-</sup> determination. A) Experimental data for consecutive additions of S<sup>2-</sup> over SAOB medium, B) calibration plot for experimental data obtained and C) durability study for n=15 slopes and k=3 replicates obtained on different days. Mean slope value of all measurements (red line) and 3-folds the standard deviation (dashed red line).

## TABLE CAPTION

**Table 1.** Real samples analysis. Comparison between the S<sup>2-</sup> concentrations obtained with the IPSSE and with a commercial sulphur ion sensor.



**Figure 1****Figure 2**

1  
2  
3  
4  
5  
6  
7  
8  
9  
10  
11  
12  
13  
14  
15  
16  
17  
18  
19  
20  
21  
22  
23  
24  
25  
26  
27  
28  
29  
30  
31  
32  
33  
34  
35  
36  
37  
38  
39  
40  
41  
42  
43  
44  
45  
46  
47  
48  
49  
50  
51  
52  
53  
54  
55  
56  
57  
58  
59  
60

Figure 3

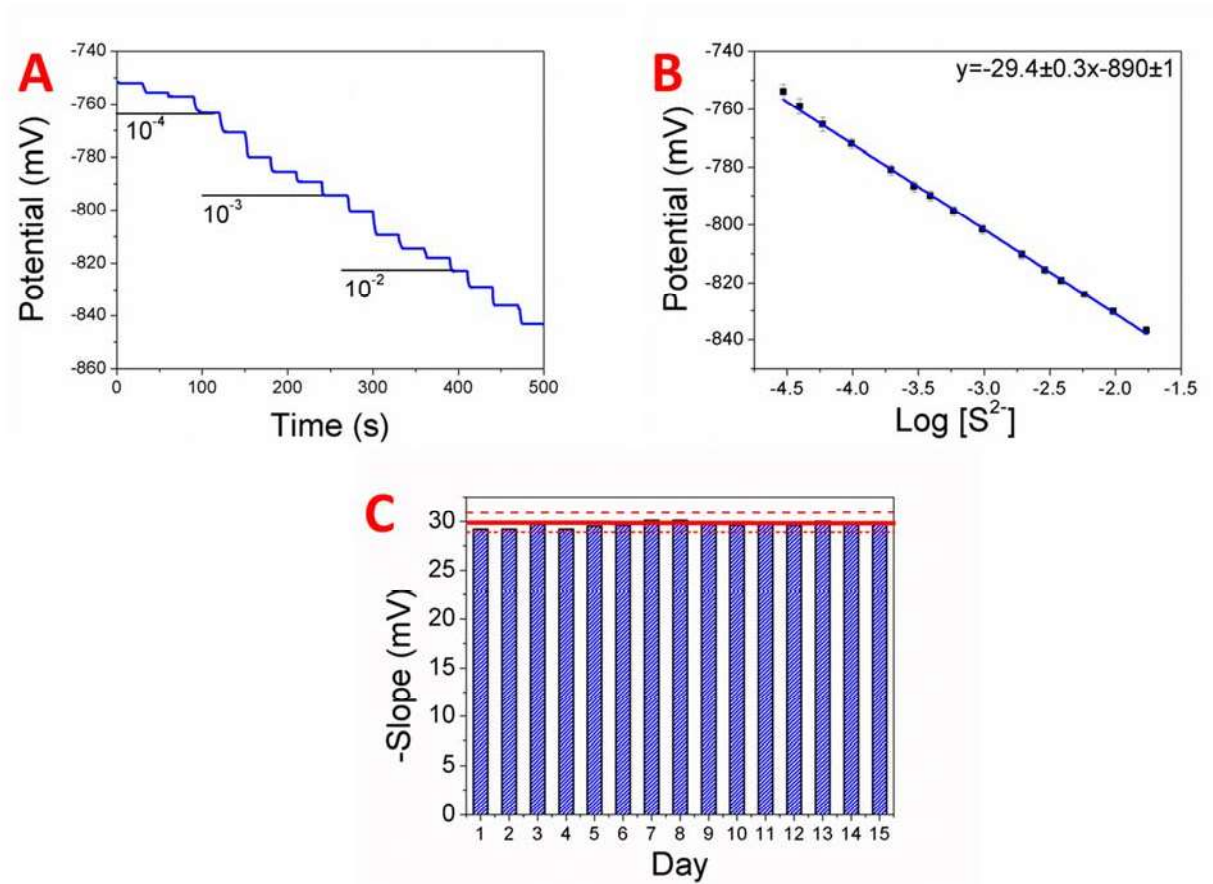


Table 1

Sample	IP SSE			Commercial		
	Mean concentration of 3 measures (mM)	Standard deviation (mM)	Recovery rate (%)	Mean concentration of 3 measures (mM)	Standard deviation (mM)	Recovery rate (%)
Reactor 1	4.44	0.55	-	5.0	0.61	-
Reactor 2	4.50	0.15	-	4.40	0.10	-
River	1.57	0.50	95	1.46	0.35	88
Sea	1.60	0.62	96	1.42	0.37	86

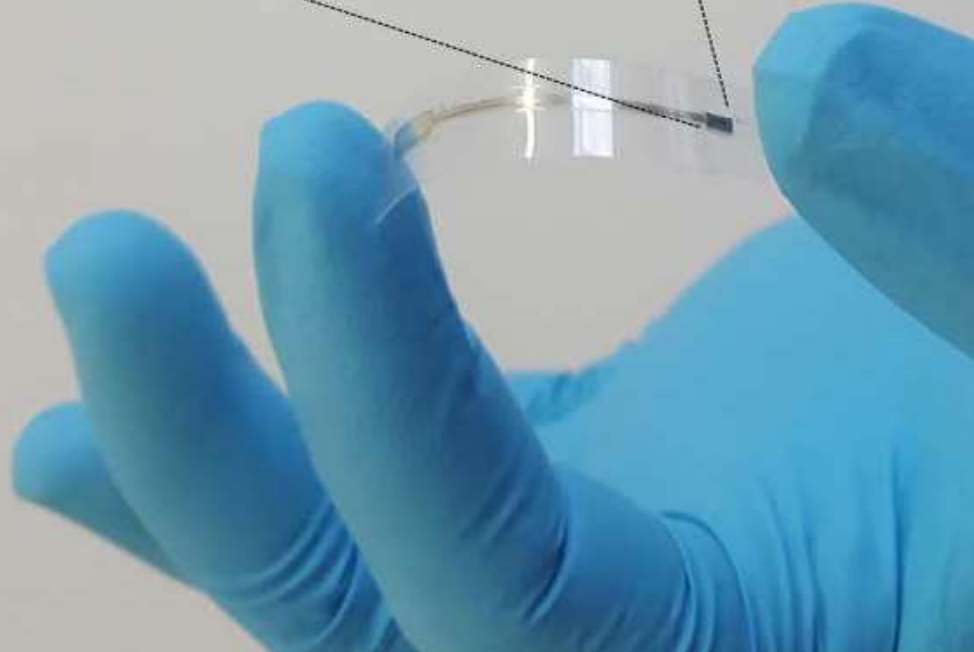
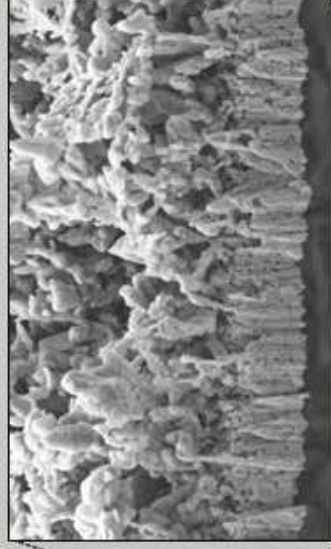
# Biotechnological



# Environmental



Ag/Ag<sub>2</sub>S



ACS Paragon Plus Environment